

Spin-Crossover Coordination Nanoparticles

Florence Volatron,[†] Laure Catala,^{*,†} Eric Rivière,[†] Alexandre Gloter,[‡] Odile Stéphan,[‡] and Talal Mallah^{*,†}*Institut de Chimie Moléculaire et des Matériaux d'Orsay (ICMMO), CNRS, Université Paris-Sud 11, 91405 Orsay, France, and Laboratoire de Physique des Solides (LPS), UMR CNRS, Université Paris-Sud 11, 91405 Orsay, France*

Received May 5, 2008

Spin-crossover coordination nanoparticles of the cyanide-bridged three-dimensional network Fe(pyrazine){Pt(CN)₄} were prepared at three different sizes using a microemulsion. The 14 nm particles present a transition centered around 265 K with a hysteresis of 6 K.

Bistable spin-crossover systems are among the most challenging in molecular chemistry because these materials can serve as components in devices for switching, signal amplification, and information storage or, as was recently reported, as efficient contrast agents.¹ Indeed, octahedral iron(II) complexes may present a spin change from a diamagnetic low-spin (LS) electronic state [$S = 0$, $^1A_2(t_{2g}^6)$] to a paramagnetic high-spin (HS) one [$S = 2$, $^5T_2(t_{2g}^4e_g^2)$] upon heating because of the larger entropy contribution of the HS state in the Gibbs free-energy variation. If intermolecular interactions are present, a cooperative process appears, characterized by a steep transition with the possible occurrence of a hysteretic behavior and thus bistability.² A large thermal hysteresis was found to be centered at room temperature in some spin-crossover systems, among which is the three-dimensional (3D) Hoffmann clathrate Fe(pyrazine){Pt(CN)₄} discovered by Real and co-workers.³ In order to study the effect of the domain size on the cooperativity of the spin-crossover transition (hysteresis and transition temperature) and thus to use these materials in information storage devices, one important goal is to synthesize controlled objects

at the nanoscale, as was successfully done on superparamagnetic and photomagnetic coordination networks.⁴ Thin films using the Langmuir–Blodgett technique were first developed on spin-crossover systems.⁵ Very recently, Bousseksou, Real, and their co-workers used the 3D Fe(pyrazine){Pt(CN)₄} network to assemble spin-crossover continuous and nanostructured multilayers on gold surfaces; objects with a size of $200 \times 200 \times 40$ nm were found to exhibit a spin change.⁶ However, unfortunately the signal of smaller objects was not detected because of the very small amount of matter present on the substrate. An alternative way to thin films is to develop the synthesis of nanoparticles in order to tune the size of the objects and to sense the magnetic and optical properties of an assembly of isolated particles prior to the investigation of the behavior of a single nanoparticle. Nanoparticles of two iron triazole systems were reported.⁷ Thermal hysteresis was for the first time evidenced for 20 nm particles of the one-dimensional material [Fe(Htrz)₂(trz)](BF₄) (where Htrz is triazole).^{7b}

In this Communication, we report the preliminary results on the synthesis and magnetic behavior of coordination nanoparticles of the 3D network Fe(pyrazine){Pt(CN)₄}. Some years ago, we successfully isolated 3 nm superparamagnetic particles protected by a pyridine derivative of the Prussian analogue Ni₃[Cr(CN)₆]₂·xH₂O using a microemulsion.^{4a} The same approach applied to the

* To whom correspondence should be addressed. E-mail: laurecatala@icmo.u-psud.fr (L.C.), mallah@icmo.u-psud.fr (T.M.). Tel: (+33) (0)1 69 15 47 49. Fax: (+33) (0)1 69 15 47 54.

[†] ICMMO, Université Paris-Sud 11,

[‡] LPS, Université Paris-Sud 11

- (1) (a) Zarembowitch, J.; Kahn, O. *New J. Chem.* **1991**, *15*, 181. (b) Gutlich, P.; Hauser, A.; Spiering, H. *Angew. Chem., Int. Ed.* **1994**, *33*, 2024. (c) Kahn, O.; Martinez, C. *J. Science* **1998**, *279*, 44. (d) Bonhommeau, S.; Molnar, G.; Galet, A.; Zwick, A.; Real, J. A.; McGarvey, J. J.; Bousseksou, A. *Angew. Chem., Int. Ed.* **2005**, *44*, 4069. (e) Muller, R. N.; Vander Elst, L.; Laurent, S. *J. Am. Chem. Soc.* **2008**, *125*, 8405.
- (2) Hauser, A.; Jęćić, J.; Romstedt, H.; Hinek, R.; Spiering, H. *Coord. Chem. Rev.* **1999**, *192*, 471.
- (3) (a) Krober, J.; Codjovi, E.; Kahn, O.; Groliere, F.; Jay, C. *J. Am. Chem. Soc.* **1993**, *115*, 9810. (b) Niel, V.; Martinez-Agudo, J. M.; Munoz, M. C.; Gaspar, A. B.; Real, J. A. *Inorg. Chem.* **2001**, *40*, 3838. (c) Galet, A.; Gaspar, A. B.; Munoz, M. C.; Bukin, G. V.; Levchenko, G.; Real, J. A. *Adv. Mater.* **2005**, *17*, 2949.

- (4) (a) Catala, L.; Gacoin, T.; Boilot, J. P.; Riviere, E.; Paulsen, C.; Lhotel, E.; Mallah, T. *Adv. Mater.* **2003**, *15*, 826. (b) Dujardin, E.; Mann, S. *Adv. Mater.* **2004**, *16*, 1125. (c) Catala, L.; Mathoniere, C.; Gloter, A.; Stephan, O.; Gacoin, T.; Boilot, J. P.; Mallah, T. *Chem. Commun.* **2005**, 746. (d) Catala, L.; Gloter, A.; Stephan, O.; Rogez, G.; Mallah, T. *Chem. Commun.* **2006**, 1018. (e) Brinzei, D.; Catala, L.; Mathoniere, C.; Wernsdorfer, W.; Gloter, A.; Stephan, O.; Mallah, T. *J. Am. Chem. Soc.* **2007**, *129*, 3778.
- (5) (a) Soyer, H.; Mingotaud, C.; Boillot, M. L.; Delhaes, P. *Langmuir* **1998**, *14*, 5890. (b) Letard, J. F.; Nguyen, O.; Soyer, H.; Mingotaud, C.; Delhaes, P.; Kahn, O. *Inorg. Chem.* **1999**, *38*, 3020. (c) Soyer, H.; Dupart, E.; Gomez-Garcia, C. J.; Mingotaud, C.; Delhaes, P. *Adv. Mater.* **1999**, *11*, 382.
- (6) (a) Cobo, S.; Molnar, G.; Real, J. A.; Bousseksou, A. *Angew. Chem., Int. Ed.* **2006**, *45*, 5786. (b) Molnar, G.; Cobo, S.; Real, J. A.; Carcenac, F.; Daran, E.; Vien, C.; Bousseksou, A. *Adv. Mater.* **2007**, *19*, 2163.
- (7) (a) Fouché, O.; Degert, J.; Daro, N.; Forestier, T.; Desplanché, C.; Létard, J. F.; Freysz, E. European Conference on Molecular Magnetism, Tomar, Portugal, Oct 2006. (b) Coronado, E.; Galan-Mascaros, J. R.; Monrabal-Capilla, M.; Garcia-Martinez, J.; Pardo-Ibanez, P. *Adv. Mater.* **2007**, *19*, 1359.

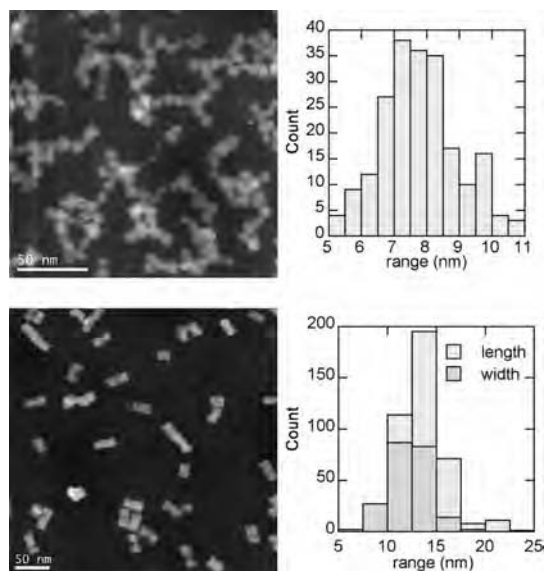


Figure 1. HAADF-STEM imaging and size distribution for **1** (top, scale bar 50 nm) and **2** (bottom, scale bar 50 nm).

$\text{Fe}(\text{pyrazine})\{\text{Pt}(\text{CN})_4\}$ network allowed the stabilization and size tuning of particles below 20 nm.

The nanoparticles were prepared by mixing two stable microemulsions: one containing the Fe^{II} salt with an excess of pyrazine and the other $\text{K}_2\text{Pt}(\text{CN})_4$ (see the Supporting Information for details of the synthesis procedure). The effect of the precursors' concentration [Fe^{II} and $\text{Pt}(\text{CN})_4^{2-}$ salts] was found to be determinant on the size of the resulting particles, as evidenced by transmission electron microscopy (TEM) imaging (Figure S1 in the Supporting Information) on particles obtained from three different concentrations, namely, 0.14, 0.08, and 0.02 mol L^{-1} . Upon a decrease in the concentration, the size of the particles increases from around 7 to 14 nm and then above 40 nm for the lowest concentration. As was expected from a nucleation-controlled process, a higher concentration of precursors induces the formation of a larger amount of nuclei and thus leads to smaller particles. High-angle annular dark-field scanning transmission electron microscopy (HAADF-STEM) imaging of the objects obtained from the two higher concentrations (noted **1** and **2** for the 0.14 and 0.08 mol L^{-1} concentrations in metal ions, respectively) confirms the quasi square shape of the particles and reveals a good size distribution for the two samples (Figure 1). In the following, we focus on samples **1** and **2** because the experiments with the lowest metal concentration lead to particles with a large size distribution that is still not perfectly controlled. The smallest particles **1** are quite monodisperse with a size (statistics performed on 212 particles) of 7.7 nm ($\sigma = 1.2$). For **2** (concentration of 0.08 mol L^{-1}), the statistics performed on 216 particles show a slight anisotropic shape with a length of 14.7 nm ($\sigma = 2.3$) and a width of 12.1 nm ($\sigma = 2.1$). An aspect ratio of 1.2 is found. No quantitative information on the thickness of the particles is available at this level of analysis yet. However, the TEM images obtained on the lowest concentration preparation show some rodlike objects with a length that corresponds to the length of the square facets and a rather homogeneous width of around 20 nm

(Figure S1c in the Supporting Information). This suggests that the particles have different orientations on the grid (parallel and perpendicular) and thus have a platelet rather than a cubic shape.

In order to recover the particles from the microemulsion, an excess of *p*-nitrobenzylpyridine (PNB) was introduced into the reaction vessel. The choice of the PNB ligand is aimed to (i) bring solubility for the particles, (ii) keep a ligand field similar to that of pyrazine, which is supposed to maintain the spin transition of the peripheral Fe^{II} ions, and, more importantly, (iii) prevent the coalescence of the particles in the solid state and thus ensure that the magnetic behavior of the studied powder samples corresponds well to individualized particles. The obtained precipitate was centrifuged, washed with acetone in order to remove the excess of the surfactant and the organic ligands, and then dried under vacuum. In the following, we focus on the samples obtained from two precursors' concentrations: 0.14 denoted **1** (7 nm particles) and 0.08 denoted **2** (14 nm particles). X-ray powder diffraction (XRPD) diagrams of the two samples correspond well to what is expected for the $\text{Fe}(\text{pyrazine})\{\text{Pt}(\text{CN})_4\} \cdot x\text{H}_2\text{O}$ network (Figure S2 in the Supporting Information). [The bulk sample was prepared by mixing in water two equimolar amounts of $\text{Fe}(\text{BF}_4)_2$ and $\text{K}_2[\text{Pt}(\text{CN})_4]$ in the presence of an excess of pyrazine. The precipitate was filtered, thoroughly washed with water, and dried under vacuum. The sample was then heated at 140 °C for 4 h. The structure of this compound consists of $\text{Fe}\{\text{Pt}(\text{CN})_4\}$ infinite layers [where each square-planar $\text{Pt}(\text{CN})_4$ molecule is surrounded by four Fe atoms and each Fe atoms is linked to four $\text{Pt}(\text{CN})_4$ molecules] connected together by the bridging pyrazine ligand that occupies the apical positions of the Fe atom to form a 3D network.] Using Scherrer's equation on single peaks gives the expected sizes of 7 and 14 nm for samples **1** and **2**, respectively. The IR spectra possess in the 2000–2200 cm^{-1} region an intense band centered at 2170 cm^{-1} corresponding to the bridging cyanide ligands (Figure S3 in the Supporting Information). A shoulder around 2140 cm^{-1} indicates the presence of nonbridging cyanides, as was expected from nanosized materials. The bands at 1420 and 1347 cm^{-1} correspond to the pyrazine and PNB ligands, respectively (Figure S3 in the Supporting Information). The relative intensity of these two bands (PNB/py) increases upon size reduction because PNB occupies only the particles' surface while pyrazine is bridging the $\text{Fe}\{\text{Pt}(\text{CN})_4\}$ layers. Elemental analysis and thermogravimetric studies allowed the determination of a unit formula for the two samples (Figure S4 in the Supporting Information). The Fe/Pt ratio was found to be equal to 1 for the two samples, while the pyrazine/PNB ratio decreased upon size reduction, as was already suggested from the IR data. These data confirm our assumption that PNB is well present on the particles' surface, protecting them from coalescence. This protecting role was further confirmed by the redispersion of the 14 nm particles in *N,N*-dimethylformamide and their observation by TEM (Figure S5 in the Supporting Information).

The magnetic behavior was investigated on the samples heated at 140 °C for 4 h to remove crystallization water

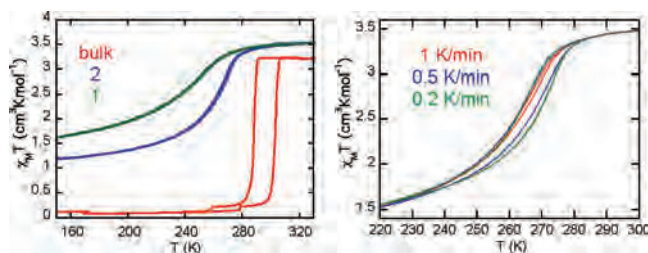


Figure 2. $\chi_{MT} = f(T)$ plots for **1**, **2**, and the bulk compound at a sweep rate of 1 K min^{-1} (left) and for **2** at three different sweep rates (right).

molecules because the transition temperature, the shape of the $\chi_{MT} = f(T)$ curves, and the width of the hysteresis loop of the bulk sample are highly dependent on the water content. XRPD diagrams before and after heating were measured and confirm that the structural integrity of the particles is conserved after the heating process (Figure S6 in the Supporting Information). The particles have a magnetic behavior different from that of the bulk (Figure 2). Upon a reduction in the size, the transition is smoother, the transition temperature shifts downward and reaches a value of 240 K for the 7 nm particles, and the hysteresis loop is narrower and almost vanishes for the smaller particles. However, for the 14 nm particles, a hysteresis with a width of 1.4 K is observed despite the rather smooth transition. The susceptibility of 14 nm particles was then measured at different temperature sweep rates (1, 0.5, and 0.2 K min^{-1}) in order to determine the hysteresis loop as close as possible to the thermodynamic equilibrium. A hysteresis loop with a width of 6.1 K was found for **2** ($T_{c2\downarrow} = 262.1 \text{ K}$ and $T_{c2\uparrow} = 268.2 \text{ K}$) at a sweep rate of 0.2 K min^{-1} . Another feature of the nanoparticles' behavior is the incompleteness of the transition; the amount of Fe^{II} ions remaining in the HS state at low temperature is larger for the smaller particles. This may be due to the fact that the peripheral Fe^{II} ions do not undergo a spin transition because the ligand field of PNB is not strong enough (see the Supporting Information).

In systems containing isolated spin-crossover molecules as in highly diluted crystals, the value of the transition temperature is defined as the ratio of $\Delta H/\Delta S$ variation between the HS and LS states at equilibrium ($\Delta G = 0$). The presence of intermolecular interactions (as in less diluted crystals) leads to an increase of the transition temperature, a change from a smooth to an abrupt transition, and eventually to the appearance of hysteresis for intermolecular interactions that are large enough.^{2,8} Such behavior was observed for the $\text{Fe}(\text{pyrazine})\{\text{Pt}(\text{CN})_4\}$ bulk compound, confirming that the transition temperature depends on the extent of the interaction between the Fe^{II} spin-crossover ions present within the network.⁹ The shift of the transition toward low temperature experimentally observed upon size reduction in the case of nanoparticles may be due to a decrease of the

cooperativity because long-range interactions are limited to the size of the particle. This hypothesis has, of course, to be confirmed. The most intriguing feature is the presence of a hysteresis loop with a width of 6.1 K despite the relatively smooth transition observed for the 14 nm particles. From the different model developed, it is well accepted that the hysteresis in spin-crossover systems occurs only for abrupt transitions.^{2,8c} In order to explain the presence of a hysteresis loop for the 14 nm particles despite the experimental smoothness of the transition, we assume that the observed behavior is dominated by the size distribution of the particles. Indeed, because the size reduction seems to shift downward the transition temperature from 265 to 240 K when the size is reduced (see above), the magnetic response of a sample that has a size distribution (even very narrow) will be smooth because the transition temperature of all of the particles cannot be the same. However, each particle undergoes an abrupt transition with a hysteresis loop, leading to the overall loop observed for the assembly of particles. Furthermore, because the particles are not strictly isolated within the sample, one cannot exclude the presence of some interparticle interaction. It is noteworthy that the recently reported $[\text{Fe}(\text{Htrz})_2(\text{trz})](\text{BF}_4)$ nanoparticles have a different behavior with almost no dependence of the abruptness of the transition on the size reduction.^{7b}

Our hypothesis succeeds in giving a reasonable explanation of the magnetic behavior observed even though the real physical origin of the transition temperature shift upon size reduction still has to be understood. Furthermore, our assumption that the individual 14 nm particles possess an abrupt transition with a thermal hysteresis loop is appealing because it opens the possibility of using these systems for information storage at the nanometric level. Investigation of the physical behavior of an assembly of well-isolated particles as performed on superparamagnetic cyanide-bridged systems is necessary to check the effect of interparticle interaction within the powder sample.¹⁰ In order to answer the questions arising from our study, the preparation of nanoparticles with larger size is underway. More importantly, their organization as monolayers on substrates, as was recently reported,¹¹ may open the way to the assessment of the behavior of a single nanoparticle.

Acknowledgment. We thank the CNRS (Centre National de la Recherche Scientifique), the EC (Contract NMP3-CT-2005-515767 NoE "MAGMANET"), and the Région Ile-de-France (Nanoscience competence center of the Région Ile-de-France C'Nano IdF) for financial support.

Supporting Information Available: Synthetic procedure, elemental analysis, TEM images, XRPD, IR spectra, and thermogravimetric studies. This material is available free of charge via the Internet at <http://pubs.acs.org>.

IC800803W

- (8) (a) Sorai, M.; Ensling, J.; Gütllich, P. *Chem. Phys.* **1976**, *18*, 199. (b) Haddad, M. S.; Federer, W. D.; Lynch, M. W.; Hendrickson, D. N. *J. Am. Chem. Soc.* **1980**, *102*, 1468. (c) Spiering, H.; Meissner, E.; Köppen, E. W.; Müller, P.; Gütllich, P. *Chem. Phys.* **1982**, *68*, 65. (d) Martin, J. P.; Zarembowitch, J.; Bousseksou, A.; Dworkin, A.; Haasnoot, J. G.; Varret, F. *Inorg. Chem.* **1994**, *33*, 6325. (9) Tayagaki, T.; Galet, A.; Molnar, G.; Munoz, M. C.; Zwick, A.; Tanaka, K.; Real, J. A.; Bousseksou, A. *J. Phys. Chem. B* **2005**, *109*, 14859.

- (10) Brinzei, D.; Catala, L.; Louvain, N.; Rogez, G.; Stephan, O.; Gloter, A.; Mallah, T. *J. Mater. Chem.* **2006**, *16*, 2593. (11) Fleury, B.; Volatron, F.; Catala, L.; Brinzei, D.; Rivière, E.; Huc, V.; David, C.; Miserque, F.; Rogez, G.; Baraton, L.; Palacin, S.; Mallah, T. *Inorg. Chem.* **2008**, *47*, 1898.